

# An hybrid finite volume - finite element method for variable density incompressible flows

Emmanuel Creusé

With C. Calgario, E. Chane-Kane and T. Goudon

Laboratoire Paul Painlevé  
Université Lille 1  
UMR CNRS 8524

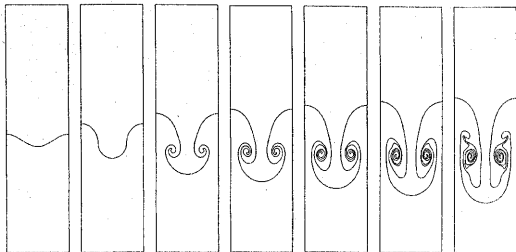
EPI Simpaf  
INRIA Lille Nord-Europe

Marseille, February 09, 2009

# Introduction

# Hydrodynamics instabilities phenomena [Try88]

- Model problem :



- At the beginning... :

- Rayleigh (End of 19th century) ;
- Taylor and Lewis (1950) ;
- Other effects : Viscosity and surface tension (Bellman-Pennington 1954), Compressibility (Mitchner-Landshoff 1964) ;
- Numerical experiments since the end of the 1960th (Harlow et Welch 1965, Daly 1967, Lugt 1983,...)

## Equations

 $\Omega \subset \mathbb{R}^2 :$ 

$$\partial_t \rho + \operatorname{div}_{\mathbf{x}}(\rho \mathbf{u}) = 0,$$

$$\partial_t(\rho \mathbf{u}) + \operatorname{Div}_{\mathbf{x}}(\rho \mathbf{u} \otimes \mathbf{u}) + \nabla_{\mathbf{x}} p - \mu \Delta_{\mathbf{x}} \mathbf{u} = \mathbf{f} ,$$

$$\operatorname{div}_{\mathbf{x}} \mathbf{u} = 0.$$

 $+B.C.$ 

- "Compressible" point of view
  - Schemes based on the transport of the quantities  $(\rho, \mathbf{u})$  ;
  - FV or FD Discretizations ;
  - The divergence constraint is imposed by a projection step or a fictitious time ;

[Goodrich-Soh 88-89, Almgren *et al* 98, Shapiro-Drikakis 05]
- "Incompressible" point of view
  - Use of a time splitting ;
  - Incompressible NS equation resolution coupled to the transport problem ;
  - Finite element discretization with stabilization for the transport ;

[Guermond-Quartapelle 00, Pyo-Shen 07]

## The approach here...

$(\rho^n, \mathbf{u}^n, p^n)$  given at time  $t^n = n \Delta t$  :

- We compute  $\rho^{n+1}$  by a FV method solution of :

$$\partial_t \rho^{n+1} + \operatorname{div}_x (\rho^{n+1} \mathbf{u}^n) = 0,$$

with B.C. for  $\rho^{n+1}$  ;

- We compute  $(\mathbf{u}^{n+1}, p^{n+1})$  by a FE method solution of :

$$\rho^{n+1} (\partial_t \mathbf{u}^{n+1} + (\mathbf{u}^{n+1} \cdot \nabla_x) \mathbf{u}^{n+1}) + \nabla_x p^{n+1} - \mu \Delta_x \mathbf{u}^{n+1} = \mathbf{f}^{n+1},$$

$$\operatorname{div}_x \mathbf{u}^{n+1} = 0,$$

with B.C. for  $\mathbf{u}^{n+1}$ .

For a better accuracy in time, we use a **Strang splitting**.

The core of the problem : The compatibility relation, which has to preserve the zero divergence constraint between all the splitting steps.

## Velocity and Pressure computation : Finite Element Method

$$\rho \in L^1(\Omega) \cap L^\infty(\Omega), \rho > 0.$$

Find  $(\mathbf{u}, p) \in (H_0^1(\Omega))^2 \times L_0^2(\Omega)$  such that :

$$\begin{cases} (\rho \partial_t \mathbf{u}, \mathbf{v}) + b(\rho \mathbf{u}, \mathbf{u}, \mathbf{v}) + a(\mathbf{u}, \mathbf{v}) + d(\mathbf{v}, p) &= (\mathbf{f}, \mathbf{v}), \\ d(\mathbf{u}, q) &= 0, \end{cases}$$

for all  $(\mathbf{v}, q) \in (H_0^1(\Omega))^2 \times L_0^2(\Omega)$ , with :

$(\cdot, \cdot)$  scalar product of  $L^2(\Omega)$  or  $L^2(\Omega)^2$ ;

$$a(\mathbf{u}, \mathbf{v}) = \mu (\nabla_{\mathbf{x}} \mathbf{u}, \nabla_{\mathbf{x}} \mathbf{v}),$$

$$d(\mathbf{v}, p) = -(p, \operatorname{div}_{\mathbf{x}} \mathbf{v}),$$

$$b(\mathbf{u}, \mathbf{v}, \mathbf{w}) = ((\mathbf{u} \cdot \nabla_{\mathbf{x}}) \mathbf{v}, \mathbf{w}),$$

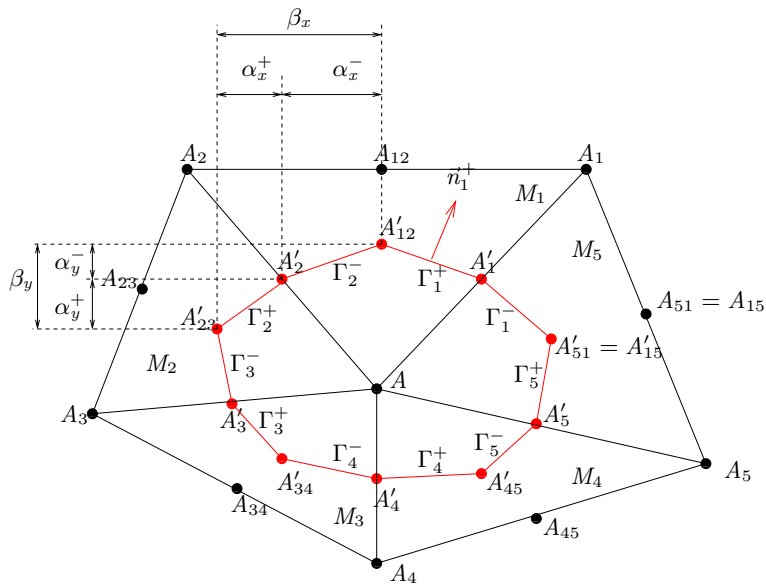
$$\mathbf{u}, \mathbf{v} \in (H_0^1(\Omega))^2;$$

$$\mathbf{v} \in (H_0^1(\Omega))^2, p \in L_0^2(\Omega);$$

$$\mathbf{u}, \mathbf{v}, \mathbf{w} \in (H_0^1(\Omega))^2.$$

$a(\cdot, \cdot)$  is coercive on  $(H_0^1(\Omega))^2$  and  $d(\cdot, \cdot)$  fulfills the LBB condition :

$$\inf_{q \in L_0^2(\Omega)} \sup_{\mathbf{v} \in (H_0^1(\Omega))^2} \frac{d(\mathbf{v}, q)}{\|\mathbf{v}\|_{(H_0^1(\Omega))^2} \|q\|_{L_2(\Omega)}} \geq \beta > 0.$$



## Space approximation

- $\mathcal{T}_h$  mesh of  $\Omega_h \subset \Omega$ , with  $h$  the space step ;
- F.E. spaces :  $\mathbf{u}_h \subset V_h \subset (H_0^1(\Omega_h))^2$ ,  $p_h \subset Q_h \subset L_0^2(\Omega_h)$  with :

$$V_h = \{\mathbf{v}_h \in \mathcal{C}^0(\bar{\Omega}_h)^2 \mid \mathbf{v}_h|_K \in \mathcal{P}^2(K) \forall K \in \mathcal{T}_h\},$$

$$Q_h = \{q_h \in \mathcal{C}^0(\bar{\Omega}_h) \mid q_h|_K \in \mathcal{Q}(K) \forall K \in \mathcal{T}_h\},$$

$$\inf_{q_h \in Q_h} \sup_{\mathbf{v}_h \in V_h} \frac{d(\mathbf{v}_h, q_h)}{\|\mathbf{v}_h\|_{(H_0^1(\Omega))^2} \|q_h\|_{L_2(\Omega)}} \geq \beta > 0.$$

- Here  $\mathcal{P}(K) = \mathbb{P}_2$  and  $\mathcal{Q}(K) = \mathbb{P}_1$ , but other choices are possible ;
- Density discretization by F.E. (i.e. polynomial on each triangle) from the V.F computed density (i.e. constant on each control volume) :

$$\rho_h \in Y_h, \text{ the natural choice being } Y_h = Q_h$$

⇒ Order 2 approximation in space

# Time approximation

F.D. discretization in time : In the interval  $(n\Delta t, (n+1)\Delta t)$ ,

- Linearization of the equations ;
- Gear type scheme (implicit, order 2) : Knowing  $\rho_h^* \in Q_h$ , find  $(\mathbf{u}_h^{n+1}, p_h^{n+1}) \in V_h \times Q_h$  such that :

$$\left( \rho_h^* \frac{3\mathbf{u}_h^{n+1} - 4\mathbf{u}_h^n + \mathbf{u}_h^{n-1}}{2\Delta t}, \mathbf{v}_h \right) + b(\rho_h^* \bar{\mathbf{u}}_h^{n+1}, \mathbf{u}_h^{n+1}, \mathbf{v}_h) + a(\mathbf{u}_h^{n+1}, \mathbf{v}_h) + d(\mathbf{v}_h, p_h^{n+1}) = (\mathbf{f}_h^{n+1}, \mathbf{v}_h),$$

$$d(\mathbf{u}_h^{n+1}, q_h) = 0,$$

for all  $(\mathbf{v}_h, q_h) \in V_h \times Q_h$  with the data  $\rho_h^* = \rho_h^n$  or  $\rho_h^{n+1}$  and  $\bar{\mathbf{u}}_h^{n+1} = 2\mathbf{u}_h^n - \mathbf{u}_h^{n-1}$ .

## Density computation : Finite Volume Method

Given  $\mathbf{u} \in (H_0^1(\Omega))^2$ , the mass equation is solved :

$$\partial_t \rho + \operatorname{div}_x(\rho \mathbf{u}) = 0,$$

in  $(n\Delta t, (n+1)\Delta t)$ , with  $\rho|_{t=n\Delta t} = \rho^n$  given.

$$\int_{\mathcal{C}_A} \partial_t \rho d\mathbf{x} + \sum_{i=1}^{nt} \left( \int_{\Gamma_i^-} \rho \mathbf{u} \cdot \mathbf{n}_i^- d\gamma(\mathbf{x}) + \int_{\Gamma_i^+} \rho \mathbf{u} \cdot \mathbf{n}_i^+ d\gamma(\mathbf{x}) \right) = 0.$$

We set  $\rho = \rho(A)$  in the control volume  $\mathcal{C}_A$  and we denote  $\mathbf{u}$  in  $\Omega$ ,  $\mathbf{u}^*$  is built on the boundary of  $\partial\mathcal{C}_A$  such that  $\mathbf{u}^* = \mathbf{u}_i^{*\pm}$  is constant on each  $\Gamma_i^\pm$ . Then :

$$\partial_t \rho_A = -\frac{1}{|\mathcal{C}_A|} \sum_{i=1}^{nt} \left( \mathbf{u}_i^{*-} \cdot \mathbf{n}_i^- \int_{\Gamma_i^-} \rho d\gamma(\mathbf{x}) + \mathbf{u}_i^{*+} \cdot \mathbf{n}_i^+ \int_{\Gamma_i^+} \rho d\gamma(\mathbf{x}) \right).$$

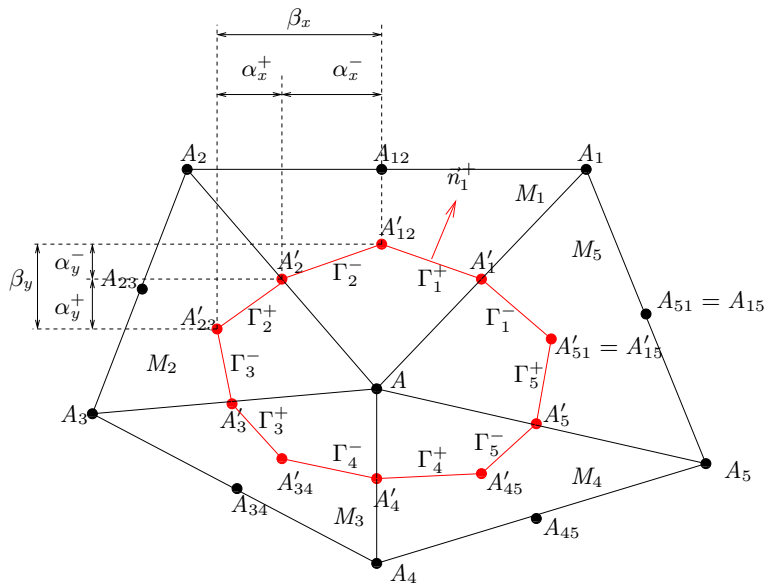
- With the knowledge of  $\rho_A|_{t=n\Delta t} = \rho_A^n$ ,  $\rho_A^{n+1}$  is computed by a RK second order scheme ;
- If we have in hand two interpolations  $\tilde{\rho}_A^\pm$  and  $\tilde{\rho}_{A_i}^\pm$  on  $\Gamma_i^\pm$ , then :

$$\int_{\Gamma_i^\pm} \rho \, d\gamma(\mathbf{x}) = \begin{cases} |\Gamma_i^\pm| \tilde{\rho}_{A_i}^\pm & \text{si } \mathbf{u}_i^{\star\pm} \cdot \mathbf{n}_i^\pm \leq 0, \\ |\Gamma_i^\pm| \tilde{\rho}_A^\pm & \text{si } \mathbf{u}_i^{\star\pm} \cdot \mathbf{n}_i^\pm > 0, \end{cases}$$

- Order 1 in space :

$$\tilde{\rho}_A^+ = \tilde{\rho}_A^- = \rho_A \text{ et } \tilde{\rho}_{A_i}^+ = \tilde{\rho}_{A_i}^- = \rho_{A_i};$$

- **Order 2 in space : MUSCL procedure**
- In the case of discontinuous solutions, we use some **flux limiters** (Van-Leer, Minmod, Superbee,..).
- Other FV methods are also possible.



# The compatibility condition

## Question

How to determine  $\mathbf{u}_i^{*\pm}$  on  $\Gamma_i^\pm$  from  $\mathbf{u}_h$  defined in  $\Omega$ ?

- The  $\mathbb{P}_2(K)$  approximation of the velocity  $\mathbf{u}_h$  fulfills the incompressibility constraint :

$$\int_{\Omega} \operatorname{div}_{\mathbf{x}} \mathbf{u}_h \psi_A \, d\mathbf{x} = 0,$$

with  $\Psi_A \in \mathbb{P}_1$  basis function of  $Q_h$ .

- But for a constant density, the mass conservation becomes :

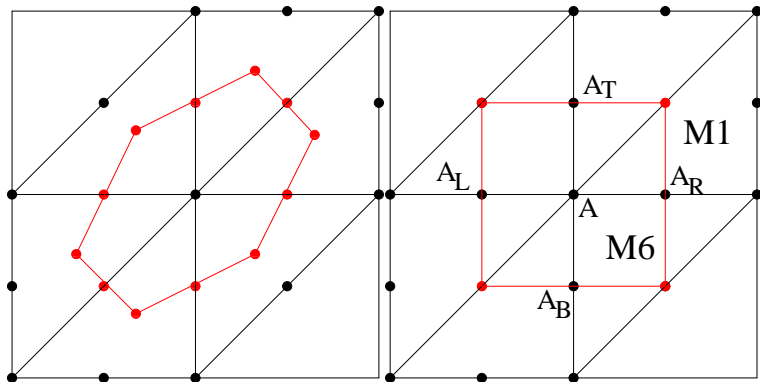
$$\sum_{i=1}^{nt} \left( \mathbf{u}_i^{*-} \cdot \mathbf{n}_i^- |\Gamma_i^-| + \mathbf{u}_i^{*+} \cdot \mathbf{n}_i^+ |\Gamma_i^+| \right) = 0,$$

- By identification, we arrive at :

$$\begin{aligned} \mathbf{u}_i^{*+} &= \frac{1}{3} (\mathbf{u}'_i + \mathbf{u}_{i,i+1} + \mathbf{u}'_{i+1}), \\ \mathbf{u}_i^{*-} &= \frac{1}{3} (\mathbf{u}'_{i-1} + \mathbf{u}_{i-1,i} + \mathbf{u}'_i). \end{aligned}$$

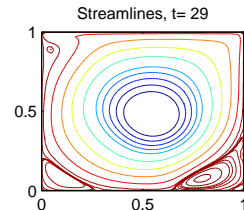
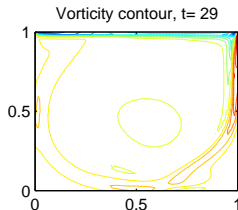
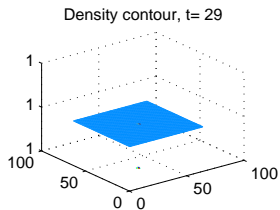
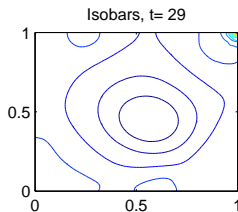
- Remark : It corresponds to the averaged velocity on the triangle

## A variant



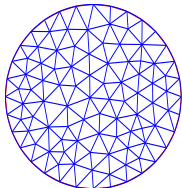
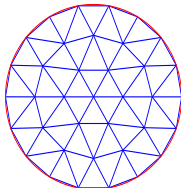
$$u_R^* + v_T^* - u_L^* - v_B^* = 0 \Rightarrow u_R^* = \frac{1}{2}(u_{M1}^* + u_{M6}^*). \text{ (the same for } v_T^*, u_L^*, v_B^*)$$

# Numerical test 1 : The driven cavity



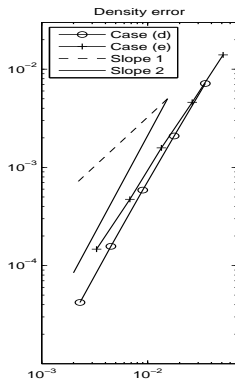
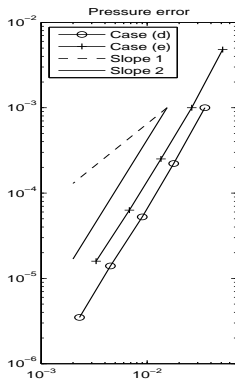
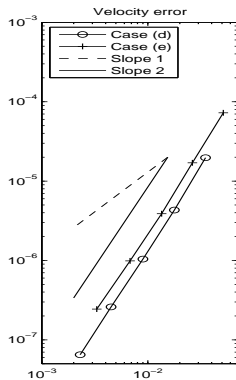
## Numerical test 2 : Rates of convergence

$$\begin{cases} \rho_{\text{ex}}(t, x, y) &= \rho_1(r, \theta - \sin t), \\ \mathbf{u}_{\text{ex}}(t, x, y) &= \begin{pmatrix} -y \cos t \\ x \cos t \end{pmatrix}, \\ p_{\text{ex}}(t, x, y) &= \sin x \sin y \sin t. \end{cases}$$



Max on  $[0, T]$  of the errors for the velocity  $\|\mathbf{u} - \mathbf{u}_h\|_{(L^2(\Omega))^2}$ , the pressure  $\|p - p_h\|_{L^2(\Omega)}$  and in density  $\|\rho - \tilde{\rho}_h\|_{L^1(\Omega)}$  by a linear reconstruction on each control volume  $\mathcal{C}_i$  around  $A_i(\mathbf{x}_i, \mathbf{y}_i)$  :

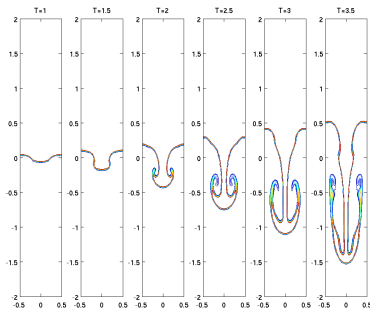
$$(\tilde{\rho}_h)_i(x, y) = (\rho_h)_i + (\nabla \rho_h)_i \cdot \begin{pmatrix} x - x_i \\ y - y_i \end{pmatrix}.$$



# Numerical test 3 : The Rayleigh-Taylor instability

## DATA

- The fluid is initially at rest with  $\rho_M$  at the top and  $\rho_m$  at the bottom ;
- It is submitted to the gravity field :  $\mathbf{f} = \rho\mathbf{g}$ , with  $\mathbf{g} = (0, -G)$  ;
- $Re = \frac{\rho_m d^{3/2} G^{1/2}}{\mu}$  ;
- Boundary conditions on vertical walls :  $u = 0, \partial_x v = 0$ .



$$\rho_M/\rho_m = 7, Re = 1000.$$

## Numerical test 3 : The Rayleigh-Taylor instability

### Some previous results...

- Trygvasson (88)  
Non viscous case, vortex method ;
- Bell and Marcus (92)  
Viscous case, FD simulation (projection method) ;
- Guermond-Quartapelle (99)  
Viscous case, FE simulation (projection method) ;
- Fraigneau *et al* (01)  
Viscous case, FV simulation ;
- ...

## Numerical test 3 : Rayleigh-Taylor instability

### Difficulties :

- the density ratio :

$$At = \frac{\rho_M - \rho_m}{\rho_M + \rho_m};$$

- The Reynolds number (with  $t = t' \sqrt{d/At G}$ )

$$Re = \frac{\rho_m d^{3/2} G^{1/2}}{\mu};$$

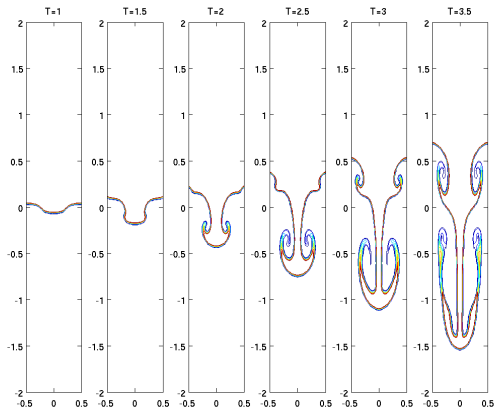
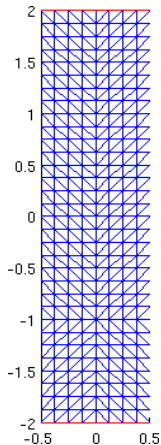
- The simulations are very sensitive to :

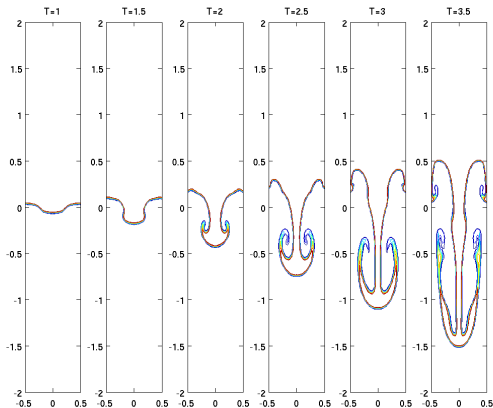
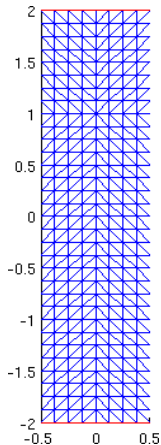
- The mesh orientation ;
- The gravity term evaluation  $\mathbf{f} = \rho \mathbf{g}$ , where  $\mathbf{g} = (0, -G)$ .

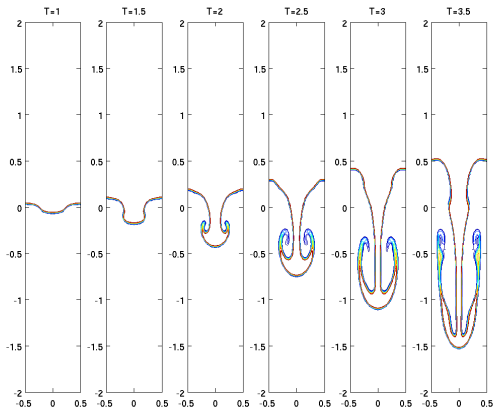
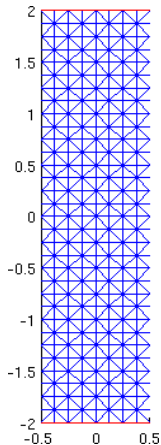
We use a piecewise  $\mathbb{P}_0$  interpolation of the density :

$$f_2 = -\frac{\rho_+ + \rho_-}{2} G,$$

with  $\rho_+$  et  $\rho_-$  the extremum values on each triangle.

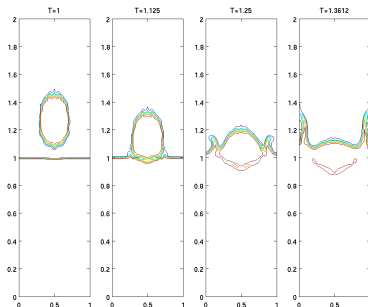
$Re = 1000, At = 0.75$ . Mesh influence

$Re = 1000, At = 0.75$ . Mesh influence

$Re = 1000, At = 0.75$ . Mesh influence

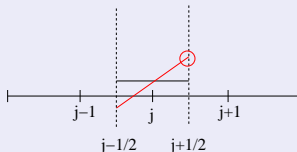
# Numerical test 4 : The falling bubble

$$Re = 3132 - \text{Density ratio} = \rho_M/\rho_m=100$$



# Flux Limiters

## 1D-analysis



- $\rho_j^+ = \rho_j + L_j \frac{\Delta x}{2}$  on  $]x_{j-\frac{1}{2}}, x_{j+\frac{1}{2}}[$ ;
- $L_j = \frac{\rho_{j+1} - \rho_j}{\Delta x} \rightarrow$  LW and loss of the maximum property principle;
- So we use for example  $L_j = \frac{1}{\Delta x} \minmod(\rho_{j+1} - \rho_j, \rho_j - \rho_{j-1})$ ;

## Multi-D + Fully unstructured meshes + High density ratios

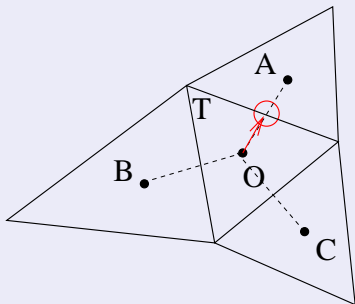
- Strong instabilities appear, because the local maximum principle is no more ensured by the finite volume scheme in the vicinity of the interface.
- Which is a well-known phenomenon for the use of a 1D limiter in a multidimensional context ([Goodman-Leveque, 1985](#)).

# Flux Limiters : Some Solutions

## Cell-centered context : Multidimensional and Monoslope limiter

- $\rho_{OA} = \rho_O + \alpha_O \underline{G}_O \cdot \underline{OA}$
- $\underline{G}_O$  is a gradient to be chosen...
- $\alpha_O$  is the flux limiter...

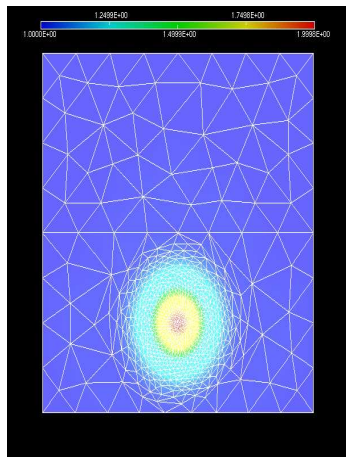
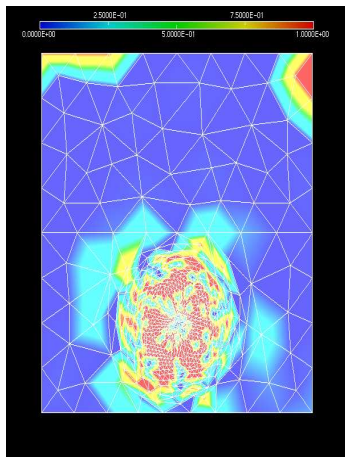
which has to ensure a **convex reconstruction** at each interface;

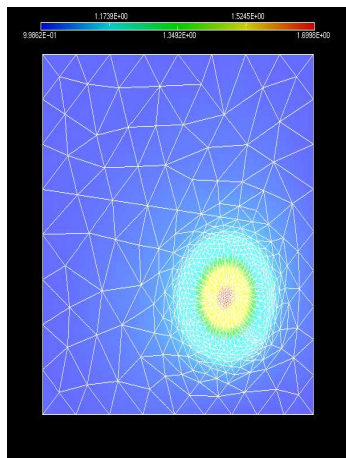
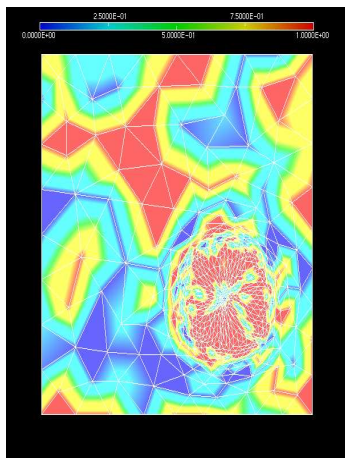


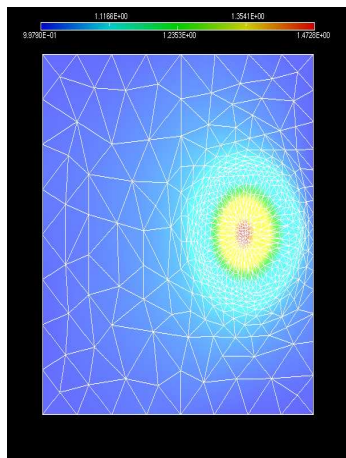
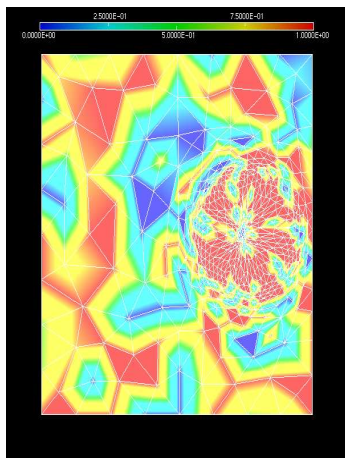
- Under a given CFL, the local maximum principle is then ensured (Batten et al 96), with further improvements (Hubbard 99);
- The **conservativity property** of the reconstruction is a fundamental property to fulfill :

$$\int_T \underline{G}_O \cdot \underline{OM} \, dx \, dy = 0, \quad M \in T.$$

## Mesh refinement : Gaussian transport - Multi D - monoslope limiter

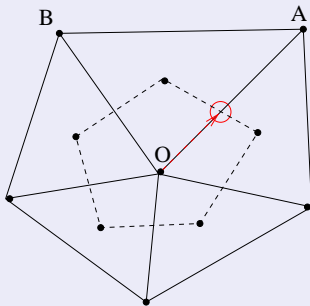






# Flux Limiters : Some Solutions

## Vertex-Based context

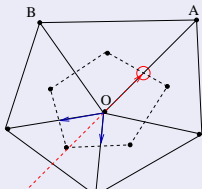


- If  $G_O$  is chosen constant, the conservativity property of the reconstruction **can no more be ensured** because of the geometry of the control volume associated to the unknown  $\rho_O$  ;
- So... we have to consider a **multislope method** : The gradient used for the reconstruction depends on the interface chosen.

# Flux Limiters : Some Solutions

## Multi-D analysis... but 1D limiter!

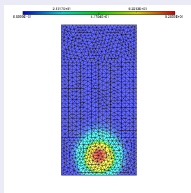
- Cell-centered analysis was very recently successfully performed (Clain and Buffard 08, Clauzon Ph-D 08);
- The proof relies in particular on :
  - The use of a monotone numerical flux;
  - A convex reconstruction at each interface;
  - The "Chainais-Hillairet" assumption :
    - Some geometrical assumptions on the mesh;
    - At a given interface, the upstream directional gradient used in the limitation process has to be chosen as a particular linear combination of the two downstream gradients related to the two other interfaces;
    - The limiter has to be a "Q limiter" ( $\psi(r) \leq \tau_{lim} r$ , OK for minmod limiter);
- All this strategy can be adapted to the vertex-based approach!



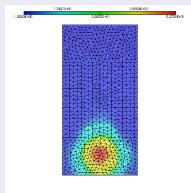
# Numerical simulations

Falling bubble with constant velocity  $u = (0, -1)^t$ ,  $T = 1.5$

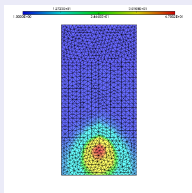
Ratio density 1/100 ; fully unstructured mesh.



1D limiter



2D monoslope limiter



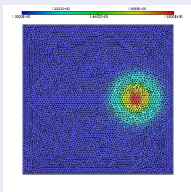
2D multislope limiter

min at $dt$	0.852309	0.987069	1.000000
max at $dt$	101.286222	100.001005	100.000000
min at $T$	0.868988	1.000000	1.000000
max at $T$	82.659262	52.770913	47.829950

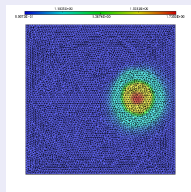
# Numerical simulations

Rotating Gaussian with velocity  $u = (-y, x)^t$ ,  $T = 1.6$

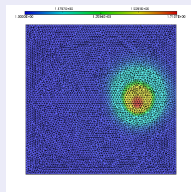
Ratio density 1/2; fully unstructured mesh.



1D limiter



2D monoslope limiter



2D multislope limiter

$L_1$ cv rate	1.92	0.97	0.93
---------------	------	------	------

Better accuracy is achieved by using :

- A reconstruction at the **middle** point on each interface ;
- A **less dissipative** limiter ;

→ Order around 1.30 can be expected.

## Further objectives...

- Improve the modelisation (surface tension) as well as the resolution (interface tracking) of the phenomenon ;
- Work with another constraint for the velocity divergence :

$$\begin{cases} \partial_t \rho + \operatorname{div}_{\mathbf{x}}(\rho \mathbf{u}) = 0, \\ \partial_t(\rho \mathbf{u}) + \operatorname{Div}_{\mathbf{x}}(\rho \mathbf{u} \otimes \mathbf{u}) + \nabla_{\mathbf{x}} p - \mu \Delta_{\mathbf{x}} \mathbf{u} = \mathbf{f}, \\ \operatorname{div}_{\mathbf{x}} \mathbf{u} = \Delta_{\mathbf{x}} F(\rho). \end{cases}$$

- **Low-Mach models** :  $F(\rho) = 1/\rho$   
Ex. Combustion models (Majda, Lions), fire propagation in a tunnel (Gasser-Struckmeier-Teleaga)
- **Mixing models (Fick law)** :  $F(\rho) = \log(\rho)$   
Ex. pollutant in a compressible fluid (Franchi-Straughan), Avalanches models (Etienne-Saramito et al.)
- For it, a good approximation of  $\nabla_{\mathbf{x}} \rho$  is needed : Use of high-order distribution schemes (Abgrall et al. 02, 05,...).  
Idea : Update of the density by a distribution of the flux density :

$$\Phi^K = \int_{t_n}^{t_{n+1}} \int_K (\partial_t \rho + \operatorname{div}_{\mathbf{x}}(\rho \mathbf{u})) \, \mathrm{d}\mathbf{x} \, \mathrm{d}t$$

on each node of the element  $K$ .